Available online at www.sciencedirect.com
ScienceDirect
Catalysis Today 117 (2006) 62–68
CATALYSIS TODAY
www.elsevier.com/locate/cattod

Analytical TEM observation of Au nano-particles on cerium oxide

Tomoki Akita [a,*], Mitsutaka Okumura [b], Koji Tanaka [a], Masanori Kohyama [a], Masatake Haruta [c]

[a] *Research Institute for Ubiquitous Energy Devices, National Institute of Advanced Industrial Science and Technology (AIST), Midorigaoka1-8-31, Ikeda 563-8577, Osaka, Japan*

[b] *Department of Chemistry, Graduate School of Science, Osaka University, Machikaneyama 1-1, Toyonaka 560-0043, Osaka, Japan*

[c] *Materials Chemistry Course, Faculty of Urban Environmental Sciences, Tokyo Metropolitan University, 1-1 Minami-Osawa, Hachioji 192-0397, Tokyo, Japan*

Available online 12 June 2006

Abstract

The structure changes of Au nanoparticles supported on CeO_2 were observed by using an analytical transmission electron microscope (TEM). The rapid shape change of a Au particle was observed during TEM observation, such as shrinking layer by layer down to a mono-atomic layer on the CeO_2 substrate with no large change of a contact diameter. The electron beam irradiation experiment revealed that the shape change of a Au particle is concerning with the oxidation state or the density of oxygen vacancies of CeO_2, where the rapid desorption and adsorption of oxygen and the ordering of oxygen vacancies were precisely identified. It was also found that the reduction by strong electron beam irradiation and subsequent oxidation generate the encapsulation of Au particles by CeO_{2-x}.

Keywords: Au; CeO_2; TEM; EELS; Reduction; Oxygen vacancy

1. Introduction

It was reported that Au/CeO_2 catalysts show high catalytic activity for low-temperature water gas shift reaction and CO oxidation [1–3]. The Au/CeO_2 catalysts prepared using the deposition precipitation method also show high catalytic activity for the oxidative decomposition of volatile organic compounds [4]. Recently, it was reported that atomically dispersed small Au clusters, positively charged on a CeO_2 surface, are responsible for low-temperature water gas shift reaction [5]. However, the detailed structure of Au particles on CeO_2 was not investigated directly because it is difficult to observe small Au clusters on CeO_2 by a conventional transmission electron microscopy (TEM) due to the disturbance of the diffraction and phase contrast by CeO_2 [6].

The structure of the Au/CeO_2 catalysts was observed using an analytical transmission electron microscope in our previous work [6,7]. Annular dark field scanning transmission electron microscopy (ADF-STEM) and energy dispersive X-ray spectroscopy (EDS) revealed that Au particles smaller than 2 nm in diameter were highly dispersed on the CeO_2 support [6,7]. However, the CeO_2 support, consisting of small crystalline grains with a size of approximately 10–20 nm, disturbed detailed observations of the contact interface between Au and CeO_2. Then TEM observations were performed on a model catalyst sample that was prepared using powder of larger CeO_2 grains with lower surface area and low index facets in order to study the interface structure between metal particles and CeO_2. Preferential orientation relationship between Au and CeO_2 crystals was observed by HRTEM. During the observations, we found novel structural changes of Au particles on CeO_2 crystals, namely rapid shape change and diffusion of Au particles with remaining Au mono-layers on CeO_2 [7]. It was deduced that such structural changes of Au particles depended on the changes in the oxidation state or the density of oxygen vacancies in CeO_2 support induced by electron beam irradiation. It is well-known as electron stimulated desorption that the metal oxides are reduced by electron beam irradiation with low energy [8] and high energy [9–13]. Although the reduction and oxidation conditions used

* Corresponding author. Tel.: +81 72 751 9732; fax: +81 72 751 9714.
E-mail address: t-akita@aist.go.jp (T. Akita).

0920-5861/$ – see front matter
doi:10.1016/j.cattod.2006.05.010

in the catalytic reaction are quite different from the electron beam reduction in the vacuum, it is valuable to investigate the detailed structure of Au and CeO_2 depending on the oxidation state of cerium oxide.

In the present work, we investigate the detailed atomic and electronic behavior during such structural changes of Au particles and CeO_2 induced by electron beam irradiation. We use the model structures prepared by using both CeO_2 power and poly-crystalline CeO_2 substrate. The changes in the atomic and electronic structure of Au/CeO_2 systems by electron beam reduction were investigated by analytical TEM. It should be noted that the reduction and oxidation behavior of the CeO_2 support with metal particles is generally quite important for various catalytic reactions. [14].

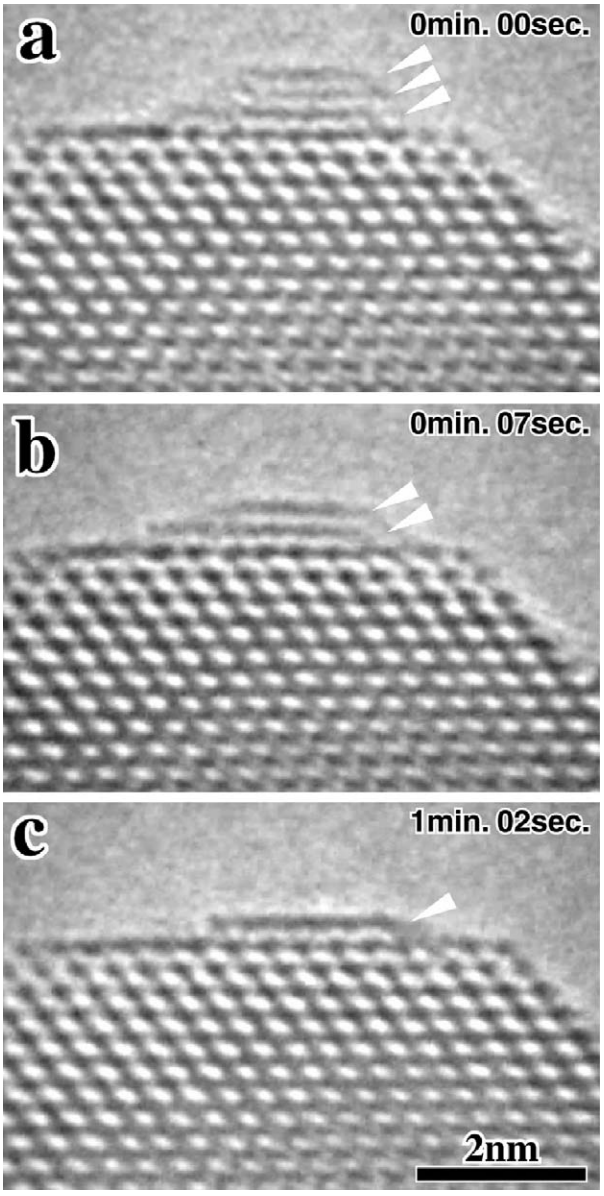

Fig. 1. A successive series of TEM images of a Au particle on CeO_2 during TEM observation. The images were recorded by VTR. The height of the Au particle is three layers (a), two layers (b) and one layer (c) as indicated by arrows.

2. Experimental

The model catalysts of Au/CeO_2 are prepared by two methods, the deposition precipitation method and vacuum deposition method. Gold nanoparticles were deposited on commercially-produced, high-purity CeO_2 powder (Kojundo Chemicals Lab. Co., purity 99.99%) using the deposition precipitation method [15], which is useful for the preparation of highly dispersed Au particles on metal oxide. The CeO_2 support was dispersed in a suitable volume of aqueous solution of $HAuCl_4$ at a fixed pH of 7. The Au content of the solution was 5.0 wt.% with respect to the weight of the CeO_2 support. The dispersion was aged at 343 K for 1 h and washed with distilled water several times. The solid material was then vacuum-dried at 0.4 Pa for 15 h at room temperature and calcinated at 673 K in air for 4 h.

The Au/CeO_2 model structure was also prepared by vacuum deposition using CeO_2 polycrystalline substrate. The tablet of CeO_2 powder (Kojundo Chemicals Lab. Co., purity 99.9%) was calcinated in air at 1773–1973 K for 12 h. The tablet of CeO_2 was cut in a disk with 3 mm in diameter. The thin CeO_2 substrate was obtained by mechanical polishing and Ar ion milling by using Gatan Pips. The thin CeO_2 substrate was calcinated at 1073 K for 4 h in order to remove the damage layer induced during preparation process. The Au particles were deposited by heating Au wires with tungsten filament in vacuum chamber at pressure of 10^{-4} Pa. The sample was set in the double tilt specimen holder for an electron microscope. A JEOL JEM-3000F transmission electron microscope was used with an accelerating voltage of 300 kV to study the Au/CeO_2 interface structure. The electron energy loss spectroscopy (EELS) measurement was also performed by Gatan Imaging Filter. The spectra were obtained in 2–4 s.

3. Results and discussion

Fig. 1 shows a successive series of TEM images of a Au particle on CeO_2 prepared by the deposition precipitation method, and reveals the typical structural change of the Au particle on CeO_2 during electron beam irradiation. The process was observed by using TV camera system and images are recorded in a video tape recorder. The small Au particle is supported on the CeO_2{1 0 0} surface. The height of the Au particle is three layers, two layers and one layer in Fig. 1a–c, respectively, as indicated by arrows. The height was decreased layer by layer during the observation as reported in previous experiment [7], and this change occurred for a few minutes. There seems to be no large change in a diameter of the contact layer. The aspect ratio of the Au particle becomes larger, which means the interface energy and/or surface energy of CeO_2 changes during the TEM observation.

It is important to investigate what really happens at the structural change of the Au particle during electron beam irradiation. The increment of the temperature is an important factor for the structural change of Au particles. The reduction of oxygen from CeO_2 support is also an important issue under electron beam irradiation. Although precise estimation of the

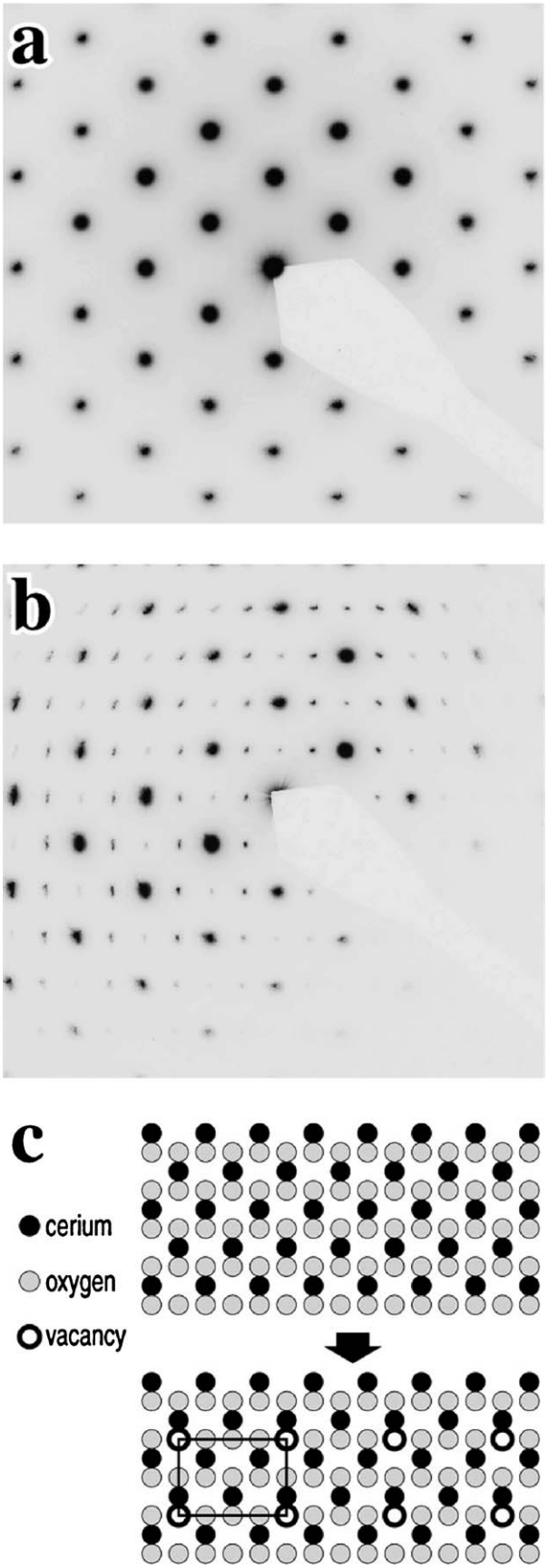

Fig. 2. Electron diffraction pattern of CeO_2 before (a) and after (b) the electron beam irradiation, and schematic drawing of structure change of CeO_2 to CeO_{2-x} having ordered oxygen vacancies (c). The drawing represent projection from $\langle 1\ 1\ 0 \rangle$ direction of CeO_2 crystal.

temperature at local area is difficult, the effect of reduction can be investigated by the electron diffraction method and EELS.

Fig. 2 shows the electron diffraction pattern obtained from $\langle 1\ 1\ 0 \rangle$ zone axis of a CeO_2 crystal grain without Au particles. Fig. 2a indicates a typical diffraction pattern of the fluorite structure of CeO_2. The extra diffraction spots are observed after the electron beam irradiation for a few minutes as shown in Fig. 2b. Long periodicity corresponding to two-fold $CeO_2\{2\ 0\ 0\}$ and four-fold $CeO_2\{2\ 2\ 0\}$ is observed. This superstructure can be attributed to the ordered vacancies of oxygen produced by the electron beam irradiation of the usual observation condition for HRTEM, through direct knock-on by high energy electrons or electron stimulating desorption [8–13]. The structure model of ordered oxygen vacancies is represented in Fig. 2c. The structure model represents the projection from $\langle 1\ 1\ 0 \rangle$ direction. The rectangle shows new unit cell of super structure created by ordered oxygen vacancies. This ordered structure of oxygen vacancies disappears after leaving the sample for 15–30 min in the electron microscope without irradiation. This means that the residual oxygen in the chamber

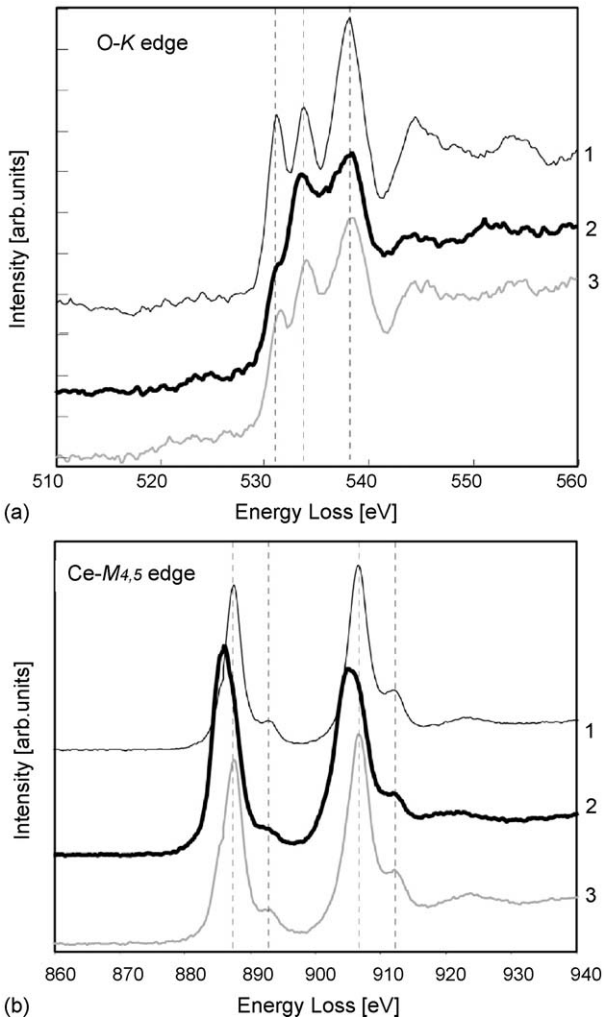

Fig. 3. EELS spectra of O-K edge (a) and Ce-M edge (b) of CeO_2. Spectrum 1 and 2 were obtained before and after the electron beam irradiation, respectively. Spectrum 3 was obtained after leaving the sample in electron microscope for 15–30 min.

of the electron microscope is absorbed again in the crystal rather rapidly even under the vacuum condition of approximately 10^{-5} Pa. The present reduced structure by the electron beam irradiation is different from the reported various reduced structure of cerium oxides prepared by high temperature reduction [16].

In order to confirm the present reduction and oxidation process of CeO_2 support, the EELS measurement was also performed. The oxidation states clearly appear in EELS spectra [9]. Fig. 3 shows the O-K edge (Fig. 3a) and Ce-M edge (Fig. 3b) of EELS spectra obtained from CeO_2 before and after the electron beam irradiation for a few minutes. In Fig. 3a, the spectrum 1 obtained before the irradiation shows three major peaks at 531, 534 and 538 eV. The intensity of the peak at 531 eV decreases by the electron beam irradiation as seen in the spectrum 2. It is considered that this peak corresponds to the

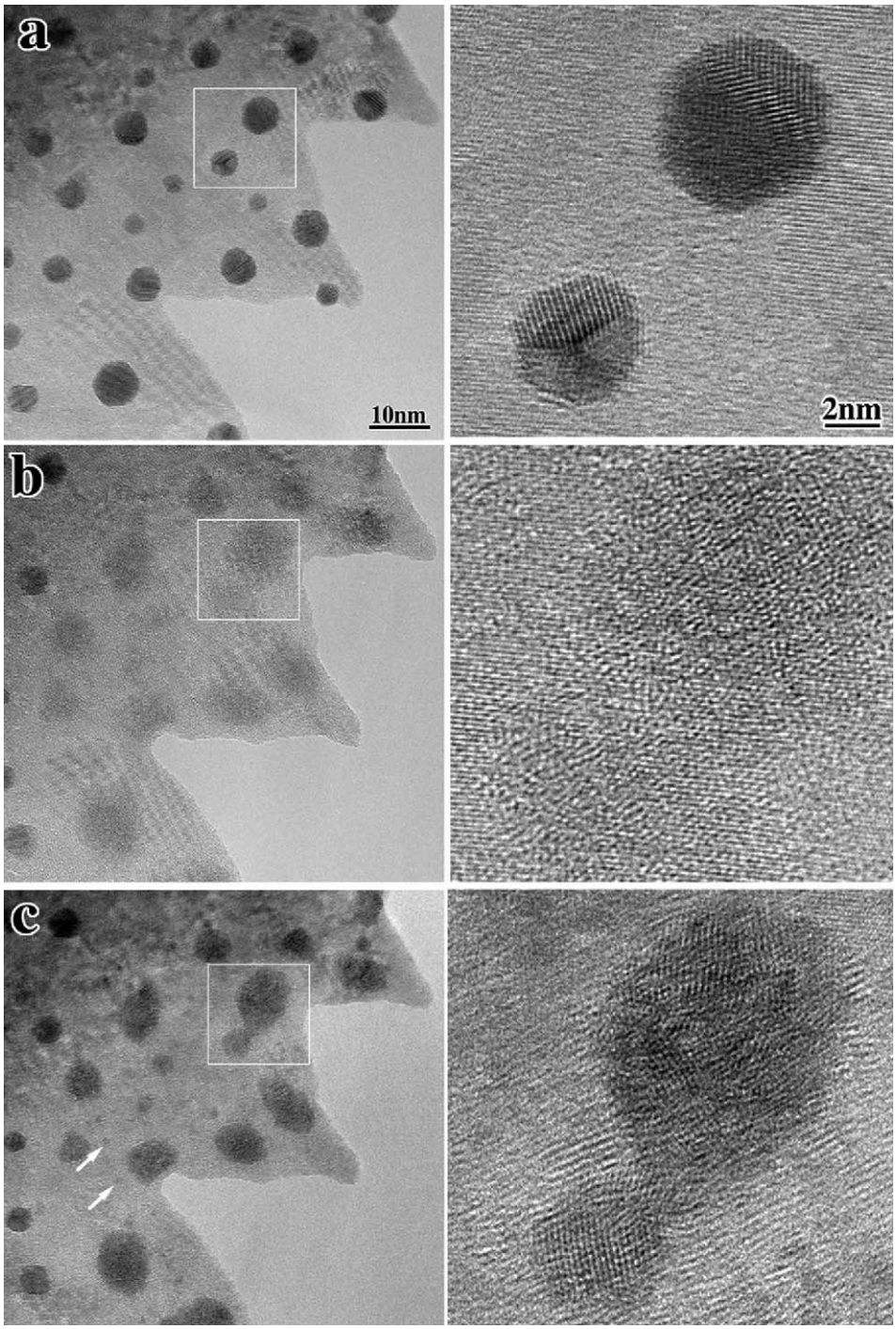

Fig. 4. TEM images of Au particles on CeO_2 before (a) and after (b) the strong electron beam irradiation. The electron beam intensity was approximately 10^7–10^8 electrons/nm^2. The image (c) was observed after 30 min leaving the sample in electron microscope. The enlarged TEM from white squares are also represented on the right side.

unoccupied Ce-4f band, strictly Ce-4f/O-2p hybridization [17]. The decrease of this peak indicates the formation of oxygen vacancies associated with the change of usual Ce^{4+} in CeO_2 with unoccupied extended Ce-4f states into Ce^{3+} with occupied localized core-like 4f state [18]. The intensity of this peak increases in the spectrum 3 again after leaving the sample in the electron microscope for 15–30 min without irradiation. The diffraction pattern also recovers to that of the original fluorite structure as shown in Fig. 2a. It should be noted that the complex behavior of Ce-4f electrons causes the variable valence number of Ce, resulting in the ease in the formation and disappearance of oxygen vacancies in CeO_2.

The reduction and oxidation of CeO_2 are also seen in Ce-M edge EELS spectra as shown in Fig. 3b. The major two peaks so called white lines are observed. The ratio of the two peaks changes by the electron beam irradiation, and the positions of the peaks also shift to lower energy region. These changes are attributed to the typical changes from Ce^{4+} to Ce^{3+} [9,19]. There seem to exist the two oxidation states of Ce^{3+} and Ce^{4+} in the spectrum 2 after the electron beam irradiation. In the spectrum 3, the peak ratio and positions almost recover to the original state after leaving the sample for 15–30 min in the electron microscope. It is interesting that the electron-beam irradiation of usual electron microscopy easily induces a lot of oxygen vacancies revealing clear ordering and that such vacancies are also immediately recovered reversibly by the residual oxygen gasses in the chamber.

Fig. 4 shows plan-view TEM images of Au particles on CeO_2 prepared by the vacuum deposition. The HRTEM images from white square areas are also shown in Fig. 4. The Au particles with 3–8 nm in diameter are observed with strong dark contrast before the strong irradiation as shown in Fig. 4a. In order to obtain a strong contrast of Au particles, the image was taken with off-Bragg condition for the CeO_2 crystal. The contrast becomes weaker after the irradiation of the strong electron beam for a few minutes as shown in Fig. 4b. The current density of electron beam is stronger than that used for a usual HRTEM observation condition, and it was estimated approximately as 10^7–10^8 electrons/nm^2. The Au particles present weak and granular contrast, indicating that the particles are not crystalline but amorphous. The Au particles should have a form of very thin layers remaining on CeO_2 surfaces after the strong irradiation as the structure of Fig. 1c, although it is not clear where the other Au atoms are located. There is a possibility of Au diffusion into bulk CeO_2 via oxygen vacancies as well as surface diffusion. About the present weak contrast of the Au particles, there is also a possibility of the Au–Ce alloy formation at Ce-rich Au/CeO_2 interfaces, which will be discussed latter.

After leaving the sample for 30 min in the electron microscope without electron beam irradiation, the contrast of Au becomes stronger again. In Fig. 4c, the Au particles have partially crystalline structure since the lattice fringes are observed in the Au particles as seen in the enlarged image

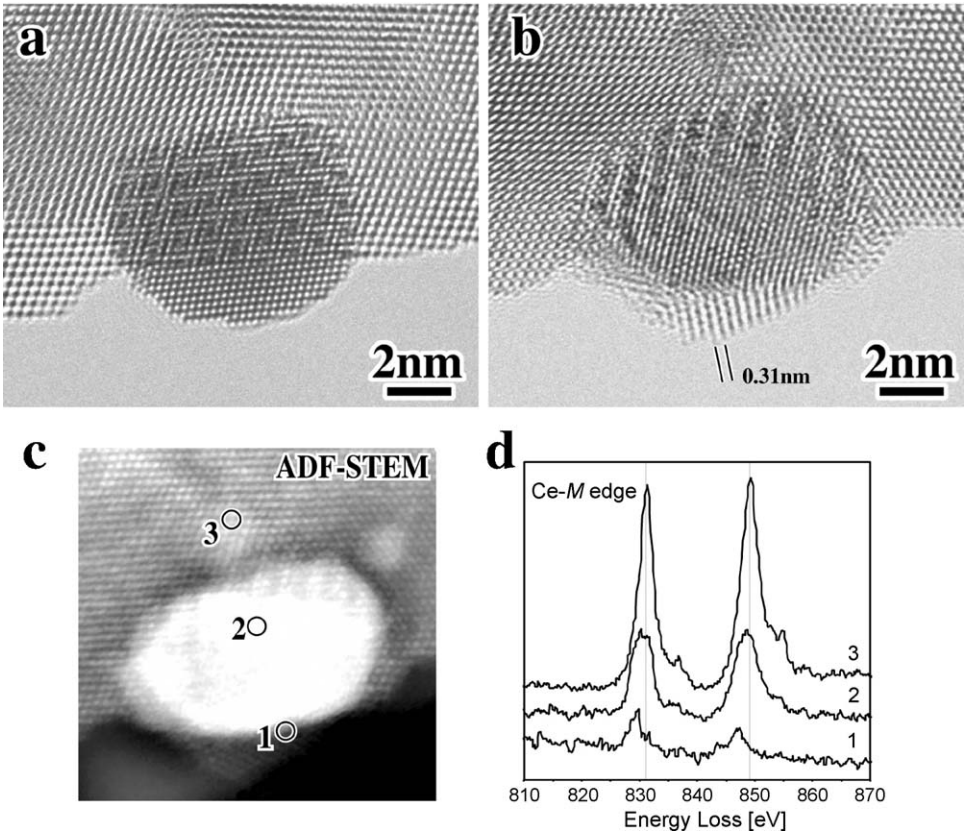

Fig. 5. TEM and ADF-STEM images of Au on CeO_2 before (a) and after (b) the electron beam irradiation and oxidation by leaving the sample for 30 min in electron microscope, and corresponding ADF-STEM image to image (b). The EELS spectra (c) obtained from each point indicated in ADF-STEM image (b).

shown in Fig. 4c. But the Au particles still include amorphous structure partially. The Au particles are relatively thin and the contact angle between Au particles and CeO_2 substrate seems smaller than that of Au particles observed in Fig. 4a, which have almost spherical shape. It can be said that each Au particle should recover its larger height via the inverse process of that in Fig. 1. The mechanism of this recovery is also not clear at present, although there is a possibility that this recovery is concerned with the simultaneous decrease of oxygen vacancies. Some Au particles disappeared by diffusion and coalescence as compared with the original structure in Fig. 4a. It is noteworthy that new small Au particles appear as indicated by arrows in Fig. 4c. The division of a Au particle occurs as observed previously [7]. This implies that it is possible to disperse Au particles in smaller particles through the present kind of phenomena under the strong reductive condition.

Fig. 5 shows the HRTEM image of a Au particle before and after the strong electron beam irradiation experiment. Fig. 5a is a TEM image before the electron beam irradiation, and Fig. 5b is taken after the strong irradiation for a few minutes and leaving the sample for 30 min in the electron microscope without irradiation. The encapsulated Au particle was obtained as observed for the Pt/CeO_2 or Rh/CeO_2 system after high temperature reduction [20,21], which is well-known as strong metal support interaction (SMSI) effect [22,23]. Fig. 5c shows an ADF-STEM image of the encapsulated Au particle corresponding to the TEM image of Fig. 5b. The Ce-M edge of EELS spectra obtained from each point indicated in Fig. 5c are represented in Fig. 5d. The surface layer covering the Au particle contains cerium atoms. Although the layer covering the Au particle is considered as CeO_2 from the space of lattice fringe of 0.31 nm corresponding to $CeO_2\{1\,1\,1\}$ in the HRTEM image in Fig. 5b, the positions of the EELS peaks indicate the cerium is not Ce^{4+} but Ce^{3+} or both mixture. It seems that the thin CeO_2 layer is immediately reduced by electron beam during a few second for EELS measurement.

Fig. 6 shows a schematic drawing of the possible process of encapsulation of a Au particle by CeO_{2-x} layers. By the electron beam irradiation, the CeO_2 substrate is reduced and the contact angle of the Au particle becomes smaller as observed in Fig. 1. This means that the adhesion energy is increased, resulting in the strong contact between Au and CeO_2 surface. The strong adhesion between metal and metal oxide by inducing oxygen defects is also theoretically predicted for Au on TiO_2 [24]. There is a possibility that the Au/CeO_2 interface or the CeO_2 region near the interface is Ce-rich under the present irradiation condition. Thus there should occur the Au–Ce alloy formation at or near the interface, due to the presence of the Au–Ce alloy phase with low melting point in the phase diagram. During the oxidation process under no irradiation, the cerium atoms segregate form the Au particle and are oxidized on the Au surface.

Of course, the reductive condition was produced by the electron beam irradiation under high vacuum in the present experiments, and it is of great interest to examine the structural changes of Au/CeO_2 systems in the reductive and oxidative conditions chemically formed via hydrogen or oxygen atmosphere in the near future. In any case, the present results provide great insights into the nature of the catalysis of Au/CeO_2 systems.

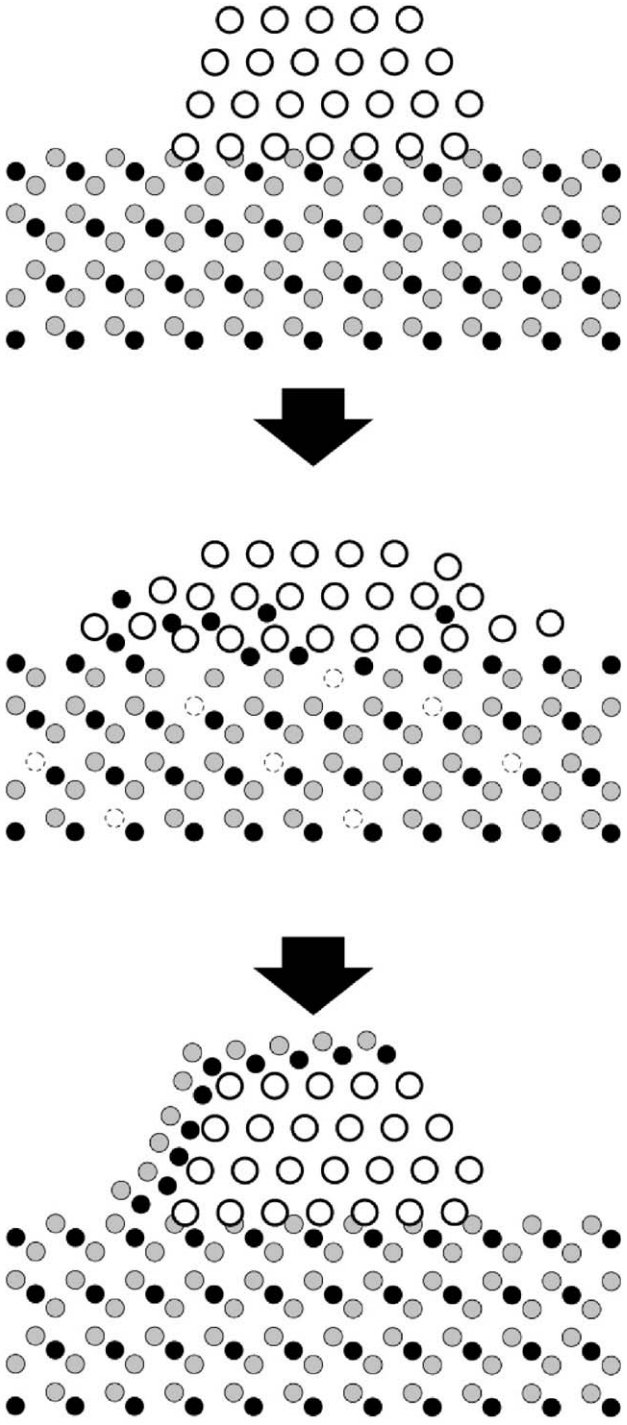

Fig. 6. A schematic drawing of the possible capsulation process of a Au particle by CeO_x layers under the electron beam irradiation.

4. Conclusion

The following conclusions have been drawn through analytical TEM study of the Au particles supported on CeO_2.

1. The reversible release and absorption process of oxygen in CeO_2 was precisely identified by the electron diffraction and EELS analyses in the electron microscope.
2. The shape change, diffusion, and recovery of Au particles depend on the oxidation state or the density of oxygen vacancies in CeO_2 substrate or surfaces. This phenomenon seems to be caused by the interface-energy change and the rapid diffusion of Au atoms associated with the rapid increase and decrease of oxygen vacancies in CeO_2.
3. The encapsulation of Au particles by CeO_{2-x} layers was produced by strong electron beam reduction. This may be caused by the Au–Ce alloy formation at the Ce-rich Au/CeO_2 interface in the reduction condition.

Acknowledgements

Part of this work was supported by the Japan Society for the Promotion of Science (JSPS-Grant-in-Aid for Scientific Research (B)). The authors are grateful to Drs. S. Ichikawa (Osaka University), K. Okazaki, and S. Tanaka (AIST) for their valuable comments and stimulating discussion. The authors are also grateful to Ms. J. Maekawa and Ms. M. Makino for their assistance with sample preparation.

References

[1] Q. Fu, A. Weber, M. Flytzani-Stephanopoulos, Catal. Lett. 77 (2001) 87.
[2] H. Sakurai, T. Akita, S. Tsubota, M. Kiuchi, M. Haruta, Appl. Catal. A: Gen. 291 (2005) 179.
[3] S. Carrettin, P. Concepciòn, A. Corma, J.M.L. Nieto, V.F. Puntes, Angew. Chem. Int. Ed. 43 (2004) 2538.
[4] S. Scirè, S. Minicò, C. Crisafulli, C. Satriano, A. Pistone, Appl. Catal. B: Environ. 40 (2003) 43.
[5] Q. Fu, H. Saltsburg, M. Flytzani-Stephanopoulos, Science 301 (2003) 935.
[6] T. Akita, M. Okumura, K. Tanaka, M. Kohyama, S. Tsubota, M. Haruta, J. Electron. Microsc. Suppl. 54 (2005) i81.
[7] T. Akita, M. Okumura, K. Tanaka, M. Kohyama, M. Haruta, J. Mater. Sci. 40 (2005) 3101.
[8] M.L. Knotek, P.J. Feibelman, Phys. Rev. Lett. 40 (1978) 964.
[9] L.A.J. Garviea, P.R. Buseck, J. Phys. Chem. Solids 60 (1999) 1943.
[10] S.D. Berger, J.M. Macaulay, L.M. Brown, Philos. Mag. Lett. 56 (1987) 179.
[11] M. Takeguchi, M. Tanaka, K. Furuya, Appl. Surf. Sci. 146 (1999) 257.
[12] D.J. Smith, L.A. Bursill, Ultramicroscopy 17 (1985) 387.
[13] M.I. BUckett, J. Strane, D.E. Luzzi, J.P. Zhang, B.W. Wessels, L.D. Marks, Ultramicroscopy 29 (1989) 217.
[14] A. Trovarelli, Catalysis by Ceria and Related Materials, Imperial College Press, London, 2002.
[15] S. Tsubota, D.A.H. Cunningham, Y. Bando, M. Haruta, in: G. Poncelt, J. Martens, B. Delmon, P.A. Jacobs, P. Grange (Eds.), Preparation of Catalysts IV, Elsevier, Amsterdam, 1995, pp. 227–234.
[16] P. Knappe, L. Eyring, J. Solid State Chem. 58 (1985) 312.
[17] Z. Hu, R. Meier, C. Schüßler-Langeheine, E. Weschke, G. Kaindl, I. Felner, M. Merz, N. Nücker, S. Schuppler, A. Erb, Phys. Rev. B 60 (1999) 1460.
[18] N.V. Skorodumova, S.I. Simak, B.I. Lundqvist, I.A. Abrikosov, B. Johansson, Phys. Rev. Lett. 89 (2002) 166601.
[19] T. Manoubi, C. Colliex, P. Rez, J. Electron. Spectrosc. Relat. Phenom. 50 (1990) 1.
[20] S. Bernal, F.J. Botana, J.J. Calvino, G.A. Cifredo, J.A. Pérez-Omil, J.M. Pintado, Catal. Today 23 (1995) 219.
[21] S. Bernal, J.J. Calvino, M.A. Cauqui, J.M. Gatica, C. Larese, J.A. Pérez Omil, J.M. Pintado, Catal. Today 50 (1999) 175.
[22] S.J. Tauster, S.C. Fung, R.L. Garten, J. Am. Chem. Soc. 100 (1978) 170.
[23] A.D. Logan, E.J. Braunschweig, A.K. Datye, D.J. Smith, Langmuir 4 (1988) 824.
[24] K. Okazaki, Y. Morikawa, S. Tanaka, K. Tanaka, M. Kohyama, Phys. Rev. B 69 (2004) 235404.